Formation of radially and azimuthally polarized light using space-variant subwavelength metal stripe gratings

Ze'ev Bomzon,[a] Vladimir Kleiner, and Erez Hasman
Optical Engineering Laboratory, Faculty of Mechanical Engineering, Technion-Israel Institute of Technology, Haifa 32000, Israel

(Received 19 April 2001; accepted for publication 18 July 2001)

We present a unique method for converting circularly polarized light into radially and azimuthally polarized beams. The method is based on the use of computer-generated space-variant subwavelength metal stripe gratings. The elements were realized on GaAs substrates and produced beams with high polarization purity at a wavelength of 10.6 μm. As a result of the conversion, the beams also undergo space-variant phase modification, which has an effect on their propagation. We demonstrate the effect experimentally, and calculate it using full space-variant polarization and phase analysis based on rigorous coupled-wave analysis and Jones calculus. © *2001 American Institute of Physics.* [DOI: 10.1063/1.1401091]

Radial and azimuthal polarized beams possess a high degree of symmetry, which has lead to their exploitation for improving such applications as particle acceleration[1] and atom trapping, optical tweezers, material processing,[2] and tight focusing.[3] In the past, such beams were created by interferometically combining two linearly polarized laser beams,[4] or by intracavity coherent summation of two orthogonally polarized TEM_{01} modes.[5] Unfortunately, these methods are somewhat cumbersome and require a high degree of coherence and interferometric stability.

In this letter, we present a method for forming azimuthal and radial polarized light using computer-generated space-variant subwavelength metal stripe gratings. Our design procedure, which is based on rigorous coupled-wave analysis (RCWA),[6] enables absolute control of the local azimuthal angle of the transmitted beam, thus enabling us to achieve high space-variant polarization purity. Furthermore, our method ensures the continuity of the grating, thereby guaranteeing the continuity of the electromagnetic field of the resulting beam.

We show that when a wave front undergoes such manipulation it is also subject to space-variant phase modification, which can be used to form either axially symmetric in-phase polarization for which the far-field image exhibits a bright center, or axially symmetric antiphase polarization for which the far field exhibits a dark center. We demonstrate these effects experimentally by converting circularly polarized CO_2 laser radiation at a wavelength of 10.6 μm into both radially and azimuthally polarized beams, which we examine in the near and far fields. We also performed a full space-variant polarization and phase analysis of the resulting beams based on RCWA and Jones calculus.[7]

Figure 1 illustrates in-phase [Figs. 1(a) and 1(c)] and antiphase [Figs. 1(b) and 1(d)] radial and azimuthal polarization, with continuous electromagnetic fields. In Figs. 1(a) and 1(c), the fields at opposite sides of the center are in phase, and at any given instance the electric fields at those points are of equal magnitude and are oriented in the same direction. This is as opposed to the fields in Figs. 1(b) and 1(d), for which the electric fields at opposite sides of the circle are antiphase. At any given instance they possess the same magnitude and are oriented in opposite directions. Due to the symmetry of the beams, it is clear that the dark center of the antiphase polarization is conserved during propagation, as opposed to the in-phase polarization, which can be expected to display a bright center in the far field. Both types of polarization can be produced by use of space-variant subwavelength metal stripe gratings and appropriate phase elements.

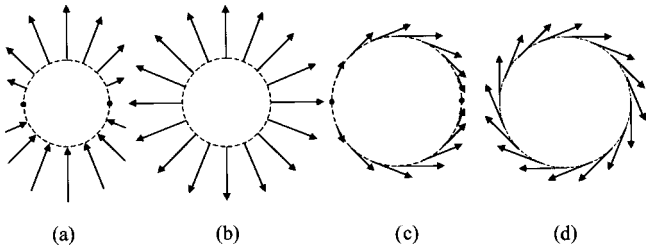

FIG. 1. In-phase radial (a) and azimuthal (c) polarization as opposed to antiphase radial (b) and azimuthal (d) polarization.

Space-variant subwavelength metal stripe gratings are typically described by a grating vector,

$$\mathbf{K}_g = K_0(r,\theta)\cos[\beta(r,\theta)]\hat{\mathbf{r}} + K_0(r,\theta)\sin[\beta(r,\theta)]\hat{\theta}, \quad (1)$$

where $\hat{\mathbf{r}}$ and $\hat{\theta}$ are unit vectors in polar coordinates, $K_0 = 2\pi/\Lambda(r,\theta)$ is the local spatial frequency for a grating of local period $\Lambda(r,\theta)$, and $\beta(r,\theta)$ is the local direction of the vector, chosen so that it is perpendicular to the metal stripes. When the period of the grating is much smaller than the incident wavelength, then only light polarized perpendicular to the wires is transmitted, and the resulting beam is linearly polarized. However, as the period of the grating increases the extinction ratio decreases. Therefore, if we assume incident circularly polarized light, the transmitted wave front will not generally be linearly polarized but rather possess elliptic polarization, with the azimuthal angle of the ellipse at a period-dependent angle $\Delta\psi(K_0)$ to the grating vector.[8] Conse-

[a]Electronic mail: zbomzy@tx.technion.ac.il

quently, in order to obtain a local azimuthal angle of $\psi_{\text{desired}}(r,\theta)$, the grating angle must be chosen so that

$$\beta(r,\theta)=\psi_{\text{desired}}(r,\theta)-\Delta\psi(K_0(r,\theta)). \tag{2}$$

Note that $\Delta\psi(K_0)$ not only depends on the period of the grating but also on other parameters such as the structure duty cycle and the substrate on which the grating has been constructed and can be calculated numerically using RCWA.

We applied Eq. (2) to the design of gratings for converting circular polarization into radially and azimuthally polarized beams. We demonstrate the design for producing radial polarization, i.e., $\psi_{\text{desired}}=0$. Applying this to Eqs. (1) and (2), and then requiring that $\mathbf{K}_g$ is a conserving vector, i.e., $\nabla\times\mathbf{K}_g=0$ leads to the self-containing differential equation for the radial element,

$$\frac{\partial}{\partial r}\{-rK_0(r,\theta)\sin[\Delta\psi(K_0(r,\theta))]\} - \frac{\partial}{\partial\theta}\{K_0(r,\theta)\cos[\Delta\psi(K_0(r,\theta))]\}=0, \tag{3}$$

from which $K_0(r,\theta)$ can be determined. By requiring that the grating vector be a conserving vector, we not only guarantee that the polarization of the resulting beam is continuous, but also ensure that the electromagnetic field defined by its local polarization and phase is continuous, thereby eliminating diffraction associated with discontinuity of the wave front.

Solving Eq. (3) by separation of variables, and by requiring that $K_0(r,\theta)$ is real, we find that the period is independent of θ and that $K_0(r)$ can be found from the transcendental equation

$$K_0(r)=K_0(r_0)\frac{r_0}{r}\frac{\sin[\Delta\psi(K_0(r_0))]}{\sin[\Delta\psi(K_0(r))]}, \tag{4}$$

where r_0 and $K_0(r_0)=2\pi/\Lambda_0$ are constants of integration that determine the geometry and local period of the grating. Using RCWA, we calculated $\Delta\psi(K_0)$ for a grating whose metal stripes consisted of 70 nm of gold on a GaAs substrate with a duty cycle of 0.5, and then numerically solved Eq. (4) using this function. Note that we experimentally verified the calculation of $\Delta\psi(K_0)$ in our previous letter.[8] Once Eq. (4) had been solved, we found grating function ϕ, defined so that $\nabla\phi=\mathbf{K}_g$ by integrating $\mathbf{K}_g$ along an arbitrary path to yield

$$\phi(r,\theta)=K_0(r_0)r_0\sin[\Delta\psi(K_0(r_0))] \times\left\{\int^{r}\frac{ctg[\Delta\psi(K_0(r'))]}{r'}dr'+\theta\right\}. \tag{5}$$

Continuity of this function requires that $\phi(r,\theta)=\phi(r,\theta+2\pi)\pm 2\pi m$ (m is an integer), and therefore, $K_0(r_0)r_0\sin[\Delta\psi(K_0(r_0))]$ must be an integer, placing a restraint on the choice of r_0 and $K_0(r_0)$. The equations for the azimuthal grating can be found by applying the same procedure with $\psi_{\text{desired}}=\pi/2$. It is important to state that an accurate solution of Eqs. (4) and (5) will result in a grating which will convert circular polarization into a space-variant polarized beam for which the local azimuthal angle is exactly $\psi_{\text{desired}}(r,\theta)$ at all points. The performance of the grating is, therefore, limited only by the accuracy of the fabrication process.

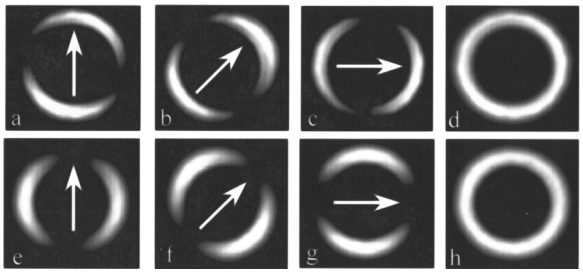

FIG. 2. Experimental intensity distributions for the radial [(a)–(d)] and azimuthal [(e)–(h)] polarizations directly after the gratings; [(a) and (e)] after passing a polarizer oriented vertically [(b) and (f)] after passing a polarizer oriented at 45°, [(c) and (g)] after passing a polarizer oriented horizontally, and [(d) and (h)] after passing a horizontal λ/4 plate and a polarizer oriented at 45°.

We realized Lee-type[9] binary metal stripe gratings for forming radial and azimuthal polarization. First, chrome masks of the gratings were fabricated using high-resolution laser lithography. These masks were then transferred onto a semi-insulating GaAs wafer 500 μm thick using photolithography, and the metal stripes were realized using a lift-off technique. The metal stripes consisted of a 10 nm adhesion layer of Ti, and 60 nm of Au. Finally, an antireflection coating was applied to the backside of the wafer. For the radial element we chose $r_0=5$ mm *and* $\Lambda_0=2$ μm, so that 3.3 mm$<r<$5 mm and 2 μm$<\Lambda<$3.2 μm, and for the azimuthal element they were $r_0=2.4$ mm and $\Lambda_0=2$ μm, so that 2.4 mm$<r<$5 mm and 2 μm$<\Lambda<$3.16 μm. The geometry of the gratings was designed so that the maximum period does not exceed the Wood anomaly in GaAs.[8]

In order to test the polarization of the beam transmitted through the gratings, we illuminated them with circularly polarized light at a wavelength of 10.6 μm from a CO_2 laser, and made four measurements of the transmitted intensity. The measurements for both the radial and azimuthal polarizations are displayed in Fig. 2. The first three were made after passing the light through a polarizer oriented vertically [Figs. 2(a) and 2(e)], diagonally at 45° [Figs. 2(b) and 2(f)] and horizontally [Figs. 2(c) and 2(g)], and the fourth measurement involved passing the light through a quarter-wave plate with its fast axis at 0° and then through a polarizer at 45° [Figs. 2(d) and 2(h)]. The intensity measurements were computed by imaging the grating through a lens onto a Spiricon PyrocamI pyroelectric camera, and the arrows in the pictures indicate the transmission axis of the polarizer for each measurement. The four measurements were then used to calculate the Stokes parameters, (S_0,S_1,S_2,S_3),[7] for each point on the resulting beam, from which the local ellipticity and azimuthal angle were obtained as, $\tan(2\psi)=S_2/S_1$ and $\sin(2\chi)=S_3/S_0$. The average deviation of this angle from ψ_{desired} was 9.8° and the average ellipticity $\tan(\chi)$ was -0.12, leading to an overall polarization purity of 95.7%. For the azimuthal element we achieved a deviation from ψ_{desired} of 5.5° and an average ellipticity of $\tan(\chi)=-0.1$, leading to a polarization purity of 98.2%. The deviation from the desired polarization results mainly from an increase in

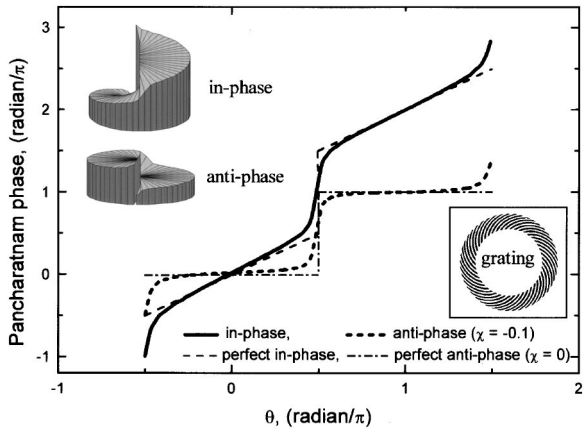

FIG. 3. Calculated Pancharatnam phase for in-phase and antiphase radial polarization formed with the computer-generated grating, as well as the phases expected from a perfect radial polarizer. The insights are three-dimensional phase distributions of the in-phase and antiphase polarizations, as well as an illustration of the geometry of the grating for forming radial polarization.

the duty cycle during fabrication, which caused a deviation of $\Delta\psi(K_0)$ from what was expected.

It remains to determine whether the resulting beam is in phase, as in Fig. 1(a), or antiphase, as in Fig. 1(b). To do this, we calculated the theoretical transmitted beam using a full space-variant polarization and phase analysis method based on RCWA and Jones calculus. The grating is represented by a space-variant Jones matrix, whose elements are calculated at each point using RCWA. Once this matrix has been calculated the resulting wave front can be found for any incident polarization. From here, we then calculated the space-variant Pancharatnam phase (based on the rule proposed by Pancharatnam for comparing the phase of two light beams in different states of polarization) of the transmitted beam as $\varphi(r,\theta)=\arg\langle\mathbf{E}(r,\theta),\mathbf{E}(R,0)\rangle$, where $\arg\langle\mathbf{E}_1,\mathbf{E}_2\rangle$ is the argument of the inner product of two Jones vectors, and $(R,0)$ are the radial coordinates of the point on the resulting beam, relative to which the phase is measured.

Figure 3 shows a calculated cross section of the Pancharatnam phase for the radially polarized beam along a concentric circle of radius $r=R=4.7$ mm, as well as the phase achieved by multiplying this beam by $e^{-i\theta}$. Since the period of the grating is independent of θ, the ellipticity, $\tan(\chi)$, of the resulting beam must be equal at all points on such circles. Calculation of the space-variant Pancharatnam phase for the beam resulting directly from our grating shows that along such curves of equal ellipticity, $\varphi=\theta-\tan^{-1}[\sin(2\chi)\tan(\theta)]$, which is equal to the area of the geodesic triangle on the Poincare sphere defined by the pole (the initial circular polarization), by $\mathbf{E}(r,\theta)$ and by $\mathbf{E}(R,0)$, and therefore, equal to the geometrical phase acquired by a beam projected through a closed loop defined by these points.[10] The phase increases linearly until $\theta=\pi/2$, where it rises sharply by π. It then continues to slowly increase until $\theta=3\pi/2$, at which an additional sharp rise occurs. The phase between $\mathbf{E}(r,\theta)$ and $\mathbf{E}(r,\theta+\pi)$ is 2π and the beam is in phase. When the beam is multiplied by $e^{-i\theta}$, we find that the phase is close to zero when $-\pi/2<\theta<\pi/2$, after which the phase suddenly jumps by π. The Pancharatnam phase between points at opposite sides of the center is now π, and the beam is antiphase. We note that for both in-phase and antiphase perfect polarizers $(\chi\to0)$, the phase jumps abruptly at $\theta=\pi/2$, causing a discontinuity in the phase function, whereas for our choice of r, $(\chi=-0.1$ rad), this transition is fast but smooth. The smoothing of the phase results from the nonzero ellipticity of the transmitted beam.

In order to verify that the beam was in phase, we measured the far-field image of the beam transmitted through the grating. The far field exhibited a clear bright spot, indicating that the beam was in phase. We then converted the polarization to antiphase by use of a spiral phase element, with a phase function $\exp[-i\theta(x,y)]$ (Ref. 11) placed after the wire grating. In this case, we observed a dark spot at the center of the beam, clearly indicative of the antiphase radial symmetry. We also obtained similar results for the azimuthal polarization.

[1] Y. Liu, D. Cline, and P. He, Nucl. Instrum. Methods Phys. Res. A **424**, 296 (1999).
[2] V. G. Niziev and A. V. Nesterov, J. Phys. D **32**, 1455 (1999).
[3] S. Quabis, R. Dorn, M. Eberler, O. Glöckl, and G. Leuchs, Opt. Commun. **179**, 1 (2000).
[4] S. Tidwell, G. H. Kim, and W. D. Kimura, Appl. Opt. **32**, 5222 (1993).
[5] R. Oron, S. Blit, N. Davidson, A. A. Friesem, Z. Bomzon, and E. Hasman, Appl. Phys. Lett. **77**, 3322 (2000).
[6] M. G. Moharam and T. K. Gaylord, J. Opt. Soc. Am. A **3**, 1780 (1986).
[7] E. Collet, *Polarized Light* (Marcel Dekker, New York, 1993).
[8] Z. Bomzon, V. Kleiner, and E. Hasman, Opt. Lett. **26**, 33 (2000).
[9] W. H. Lee, Appl. Opt. **13**, 1677 (1974).
[10] P. K. Aravind, Opt. Commun. **94**, 191 (1992).
[11] R. Oron, N. Davidson, A. A. Friesem, and E. Hasman, Opt. Lett. **25**, 939 (2000).